Lifetime measurement of the first 2^+ state in ^{178}Pt

C. B. Li (李聪博),[1] F. Q. Chen (陈芳祁),[1] X. G. Wu (吴晓光),[1,*] C. Y. He (贺创业),[1] Y. Zheng (郑云),[1] G. S. Li (李广生),[1] Q. M. Chen (陈启明),[1] Z. C. Gao (高早春),[1] Q. L. Xia (夏清良),[1] W. P. Zhou (周文平),[2] S. P. Hu (胡世鹏),[1] H. W. Li (李红伟),[1,3] J. L. Wang (汪金龙),[1] J. J. Liu (刘嘉健),[1,4] Y. H. Wu (吴义恒),[1,3] and P. W. Luo (罗朋威)[1,4]

[1]*China Institute of Atomic Energy, Beijing 102413, China*

[2]*Shenyang Institute of Engineering, Shenyang 110136, China*

[3]*College of Physics, Jilin University, Changchun 130012, China*

[4]*College of Physics and Technology, Shenzhen University, Shenzhen 518060, China*

(Received 30 June 2014; revised manuscript received 10 September 2014; published 7 October 2014)

The lifetime of the 2_1^+ state in ^{178}Pt was measured by using fast-timing techniques with the high-purity Ge and $LaBr_3$: Ce array using the ^{154}Gd(^{28}Si,4n) reaction at a beam energy of 146 MeV. The deduced $B(E2,2_1^+ \rightarrow 0_1^+)$ strength is discussed in relation to the systematics of the previously reported $B(E2,2_1^+ \rightarrow 0_1^+)$ strengths in the light even-even $^{176-184}$Pt isotopes and compared with calculations of the generator coordinate method. The present results support a configuration-mixing interpretation for low-spin states in these light Pt isotopes.

DOI: 10.1103/PhysRevC.90.047302 PACS number(s): 21.10.Tg, 23.20.Js, 25.70.Gh, 27.70.+q

The study of spectroscopic properties in many Pt isotopes has attracted considerable interest in recent years. A rich variety of shapes, concerning prolate, oblate, and triaxial deformations, as well as shape coexistence, has been seen in the Pt isotopes. Unlike the heavier mercury isotopes, where the lower-energy bands exhibit oblate-shape characteristics, and the higher-energy bands exhibit prolate characteristics, in Pt nuclei the phenomena of shape coexistence manifests itself as a mixed band instead of as different bands [1–3]. The coexistence between prolate and oblate shapes has been invoked to interpret the yrast band structures and transition probabilities [4–7] for light Pt isotopes and more detailed three-band mixing (a quasi-γ band is included) has been applied to interpret a series of decay measurements for the yrast and nonyrast states in the light Pt nuclei [8]. From a theoretical point of view, these properties have been investigated by quantum calculations in this region in terms of both microscopic calculations and phenomenological models [9–18]. There has been considerable effort to study nuclear structure properties in Pt isotopes by using both heavy-ion [19–24] and Coulomb excitation [25] experiments. Competing nuclear shapes are closely associated with the nuclear collective motion and especially quadrupole collectivity at low spin. Thus, the magnitudes of the experimental $B(E2)$ values are sensitive to the mixing configurations that determine the nuclear shape. The lifetime of the first 2^+ state in an even-even nucleus is, in general, inversely proportional to the reduced transition probability, $B(E2,2_1^+ \rightarrow 0_1^+)$, and gives a first indication of the collectivity of the nucleus. In this respect, the evolution of collectivity in Pt isotopes should bring valuable information about the shape coexistence. However, the experimental data have remained incomplete for the neutron-deficient platinum isotopes.

Excited states in the neutron-deficient isotope ^{178}Pt have previously been investigated using α- and β-delayed spectroscopy [8,26,27] which first established the level scheme of ^{178}Pt. Then, Dracoulis *et al.* [4], Soramel *et al.* [28], and Kondev *et al.* [6] respectively used ^{144}Sm(^{37}Cl,$p2n$), ^{142}Nd(^{46}Ti,$2\alpha 2n$), and ^{103}Rh(^{78}Kr,3p) heavy-ion fusion reactions populating the excited states of ^{178}Pt. They expanded considerably the level scheme and measured the lifetimes in the yrast band up to the 8^+ state, excluding the 2^+ state. In the present work, we report a measurement of the lifetime of the 2_1^+ state in ^{178}Pt. The experiment employed fast-timing techniques with the $LaBr_3$: Ce scintillator and high-purity Ge (HPGe) detector array at the China Institute of Atomic Energy (CIAE). The new data obtained in this experiment can be valuable to warrant a comprehensive study of the role of shape coexistence in Pt nuclei.

Owing to severe competition from fission and charged-particle emission, the measurements are difficult using the above reactions. We chose the more efficient 4n channel ^{154}Gd(^{28}Si, 4n) heavy-ion fusion reaction populating the excited states of ^{178}Pt. A fusion-evaporation statistical model calculation using the program CASCADE [29] predicts that ^{178}Pt is produced in this reaction with a cross section of about 200 mb; the cross sections of other products of the reaction are much lower. A 146 MeV ^{28}Si beam with an intensity of about 20 nA was used to produce the parent ^{178}Pt. The target consisted of a 0.9mg/cm^2 ^{154}Gd rolled onto a 12.5mg/cm^2 Pb backing. Measurements were performed using the $\gamma\gamma(t)$ fast-timing method. The lifetimes of levels of interest were determined by a fast-timing delayed coincidence setup consisting of six $LaBr_3$: Ce detectors working in coincidence with nine Compton-suppressed HPGe detectors. The six $LaBr_3$: Ce detectors were mounted around the target chamber on a ring of approximately 90° with respect to the beam axis. The HPGe detectors were kept at 42°, 90°, 140°, and 153° with respect to the beam direction. The details of experimental setup and data acquisition system can be found in Ref. [30].

The recently developed $LaBr_3$: Ce scintillator is becoming very popular for use in γ-ray spectroscopy measurements due to its good time resolution (a few hundreds of picoseconds), higher efficiency than a NaI detector of the same size,

*wxg@ciae.ac.cn

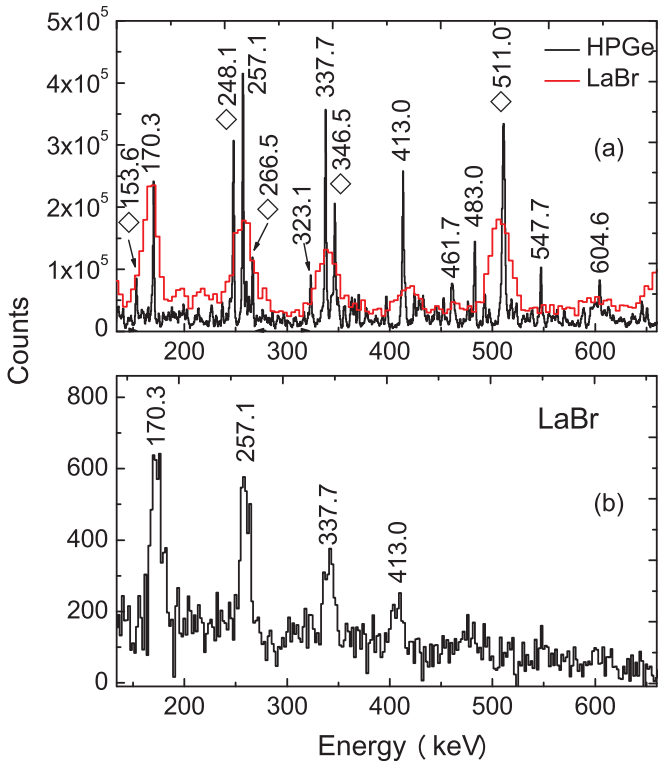

FIG. 1. (Color online) ^{178}Pt energy spectra: (a) Total projection from all HPGe and $LaBr_3:Ce$ detectors. (b) $LaBr_3:Ce$ energy spectrum gated on the sum of 337.7, 413.0, and 483.0 keV transitions in the HPGe detectors. The energies marked on the peaks are in keV. The diamond labels indicate contaminations.

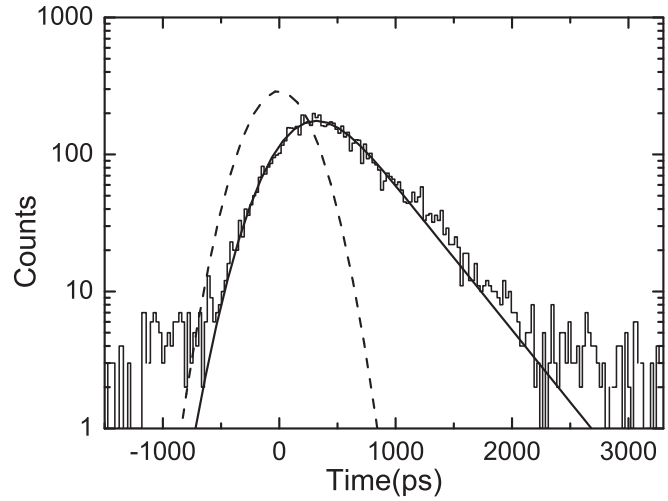

FIG. 2. Time spectrum for decay of yrast 2^+ state in ^{178}Pt measured from time difference between 170.3 and 257.1 keV transitions. The dashed line shows the Gaussian distribution (determined by gating on the Compton background near the 170.3 keV peak) which approximates the prompt spectrum. The solid line is a fit to the data.

and most importantly its energy resolution of 2.8%–3.5% at 662 keV depending on its size and purity. These good features, in fact, make this detector an alternative to a HPGe or BaF_2 detector in some applications. The fast-timing method, developed at first with BaF_2 detectors [31] knows nowadays a renewal with the discovery of $LaBr_3:Ce$ scintillators. The experimental procedures were optimized for the use of the delayed-coincidence $\gamma\gamma\gamma(t)$ method discussed in more detail in Ref. [32]. Gamma rays produced in the reaction were collected in coincidence mode, and only the $\gamma\gamma\gamma(t)$ events involving the Ge-$LaBr_3$-$LaBr_3$ detectors were useful for extracting the time spectrum. The combination of HPGe detectors and fast-response scintillator detectors allowed a high-precision selection of the desired decay scheme and, within that scheme, a desired γ-ray cascade. This vastly simplified the coincident γ-ray spectrum recorded with the $LaBr_3:Ce$ detector, and thus the γ-ray peaks of interest could be identified with high selectivity.

Figure 1(a) shows the energy total projection for the all HPGe detectors to compare the energy resolution with an energy spectrum of the $LaBr_3:Ce$ detectors in the present experiment. The energies of strong γ-ray transitions are marked on the figure. There are some transitions which lie too close in energy to be fully resolved by the $LaBr_3:Ce$ detectors. A more selective gate on spectra from the HPGe detectors can isolate the transitions in a complex peak, as illustrated in Fig. 1(b). The figure shows a coincidence spectrum produced by gating on the sum of 337.7 ($6^+ \rightarrow 4^+$), 413.0 ($8^+ \rightarrow 6^+$), and 483.0 ($10^+ \rightarrow 8^+$) keV transitions in the HPGe detectors. Compared with total projection spectra in Fig. 1(a), the main transitions of ^{178}Pt can be identified, such as the much slenderer 170.3 ($2^+ \rightarrow 0^+$) and 257.1 ($4^+ \rightarrow 2^+$) keV peaks in Fig. 1(b).

The lifetime of the first 2^+ excited state was determined from the analysis of the time spectrum shown in Fig. 2. It represents the time difference measured between the 170.3 keV transition depopulating the 2^+ state and the 257.1 keV transition feeding the state. Strong contaminant peaks were excluded from the gate; however, the background from the Compton continuum could not be fully eliminated, as shown in Fig. 1(b). Therefore, we have set a gate on the Compton spectrum just above the 170.3 keV peak and, in the process of sorting, events in the Compton gate were subtracted from the time spectrum generated by the full-peak events. The resultant time spectrum was nearly free from Compton events. It clearly shows an asymmetric contour due to a decay time larger than the width of the prompt coincidence spectrum. The time spectrum was fit with an exponential decay convoluted, as shown the solid line in Fig. 2. As the centroid and the full width at half maximum of the prompt time spectra slightly change as a function of γ-ray energy, the position and the width of the corresponding prompt curve can be also taken as the result of a free fit. In fact, we also have fit the experimental data with free parameters, and finally obtained an identical lifetime value within uncertainties. Finally, the value we adopt for the lifetime is the mean of these different fitting results and provides a lifetime of $\tau = 412\,(30)$ ps.

Using this lifetime, the mixing ratio and internal-conversion coefficient of the 170.3 keV transition as given by the Nuclear Data Sheets, we obtained the reduced transition probability $B(E2, 2_1^+ \rightarrow 0_1^+) = 143\,(10)$ W.u. for this transition. The

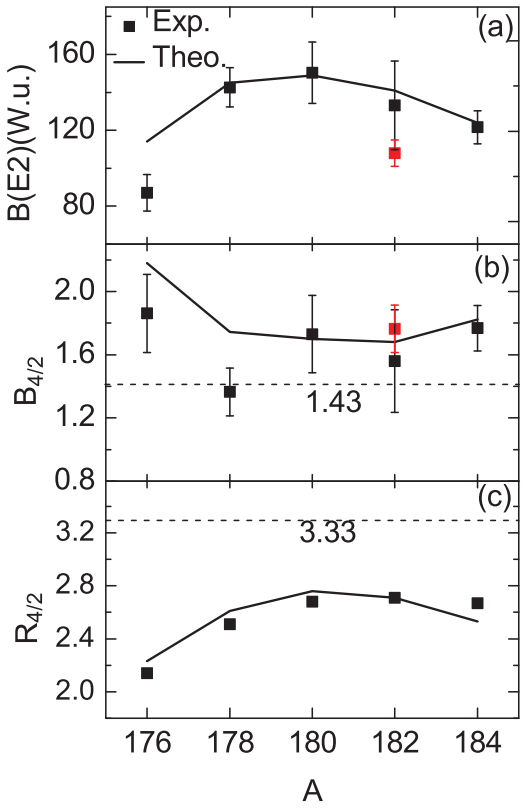

FIG. 3. (Color online) Systematics of the (a) $B(E2,2_1^+ \rightarrow 0_1^+)$, (b) $B_{4/2}$, and (c) $R_{4/2}$ values for the Pt isotopes with $98 \leqslant N \leqslant 106$. The experimental point at $N = 100$ is from the present work. Two conflicting values of $B(E2,2_1^+ \rightarrow 0_1^+)$ are plotted for ^{182}Pt corresponding to measurements from different experimental groups. The experimental data for the other nuclei are taken from the Nuclear Data Sheets. The solid lines indicate the results calculated with the generator coordinate method (see text).

systematics of the $B(E2,2_1^+ \rightarrow 0_1^+)$ values is shown for the Pt isotopes, from ^{176}Pt to ^{184}Pt, in Fig. 3(a). Our new value for ^{178}Pt is close to the maximum values found in ^{180}Pt at near neutron midshell. For ^{182}Pt ($N = 104$), the $B(E2,2_1^+ \rightarrow 0_1^+) = 133\,(23)$ W.u. reported by Walpe *et al.* [23] conflicts with the value [108 (7) W.u.] from Ref. [24]. Both lifetime values have been measured independently by using the recoil-distance method, but they cannot both be right. Although the lower data have smaller experimental uncertainty, it does not seem to follow the smooth trend of data from neighboring isotopes. In addition, we note that the value reported by Gladnishki *et al.* [24] did not use the coincidence-based differential decay curve method (DDCM) to analyze the data and thus unobserved feeding effects could contribute to the measured difference. Thus, one might be inclined to favor the higher-lying data point over the lower one, albeit the quoted uncertainties in Ref. [23] are larger. Finally, from the entire data set of even-even Pt isotopes, one can see that the value determined by the present measurement shows a relatively smooth evolution with mass, indicating an increase in the collectivity with increasing mass, reaching the expected maximum value near the neutron midshell.

As mentioned above, some light Pt isotopes around the neutron midshell are often revealed to exhibit the coexistence of prolate and oblate shapes. For comparison with experimental results, beyond-mean-field calculations were done. In the following, the excitation spectra and transition probabilities of even-mass neutron-deficient Pt isotopes, from ^{176}Pt to ^{184}Pt, were calculated within the framework of the generator coordinate method (GCM). The idea of the method can be understood as an extension to that of the "two-band mixing" method [4,33]. In the GCM calculation, many (rather than two) bands are mixed by the pairing-plus-quadrupole interaction, each with a different deformation. These bands are described by deformed BCS vacuum, projected onto good spin and particle number. More explanations on the general ideas of the method can be found in Ref. [34].

The Hamiltonian in the GCM calculation takes the following form:

$$\hat{H} = \hat{H}_0 - \frac{\chi}{2} \sum_{\mu} \hat{Q}_{\mu}^{+} \hat{Q}_{\mu} - G_M \hat{P}^{+} \hat{P} - G_Q \sum_{\mu} \hat{P}_{\mu}^{+} \hat{P}_{\mu},$$

the details of which can be found in Ref. [35]. The strength of the quadrupole-quadrupole interaction is determined by fitting the energy observed 2^+ state of the ground-state band. The monopole pairing strength G_M is $[24.42 - 15.94(N - Z)/A]/A$ MeV for neutrons, and $24.42/A$ MeV for protons. The quadrupole pairing strength $G_Q = 0.14 G_M$. The configuration space is built by 14 BCS vacuum, with either prolate or oblate deformations. General two-dimensional (β, γ) energy-map calculations verify that potential-energy surfaces (PESs) evolve from prolate shapes in the lighter isotopes ($A \approx 176$ to 184) to oblate shapes for the heavier neutron-rich isotopes ($A > 196$, until the spherical shape is reached for ^{204}Pt), connected by triaxial shapes or γ-soft for intermediate isotopes ($A \approx 186$ to 196) [5,18,36–38]. The theoretical work, therefore, suggests that, from $A = 176$ to 184, Pt isotopes could be studied by using the axial mean-field approach. Thus, in the present calculations we restrict this set to the quadrupole deformation β, triaxial shapes, i.e., the γ degree of freedom, are not considered.

Since the quadrupole moment is not a directly observable quantity, the shape evolution can be analyzed by investigating the intrinsic states in terms of the potential-energy surface of each nucleus. The energy curves obtained after projection on angular momentum $I = 0_1^+, 2_1^+, 4_1^+$ are displayed in Fig. 4. Prolate shapes correspond to $\beta > 0$, oblate shapes correspond to $\beta < 0$. For the ground state the general behavior of the projected surfaces is rather similar in the considered isotopes. There is a well-deformed prolate minimum, at $\beta \approx 0.3$, for all isotopes, becoming most pronounced around the midshell. There is also a well-defined, slightly deformed, oblate minimum for all isotopes. We find that the trend of shape changes predicted by our calculations in the considered Pt isotopes agrees well with the the conclusions extracted from the combination of the interacting boson model (IBM) plus the configuration mixing model and the Hartree–Fock–Bogoliubov using Gogny-D1S interaction [18]. For the excited 2_1^+ and 4_1^+ states, the PESs in $^{176-184}$Pt still contain a significant admixture of the oblate and prolate wells. But on

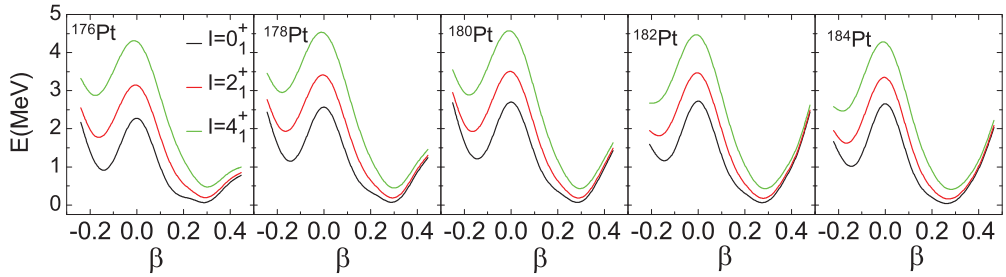

FIG. 4. (Color online) Particle-number and angular momentum $I = 0_1^+, 2_1^+, 4_1^+$ projected deformation energy curves for $^{176-184}$Pt.

the oblate side, the energy increases much faster compared to the prolate side as the increase of angular momentum, which can result in a large change of structure of the collective wave functions with spin: the higher-spin-state wave functions are much less mixed than the wave functions corresponding to lower states. Investigation of the lighter or heavier Pt isotopes, the PES results [1,2,18,36] predict a rapid change to a triaxial shape; however, is not performed in present work but could be undertaken in a forthcoming presentation.

The underlying structure of the PES described above is then reflected in the spectra calculated from configuration-mixing calculations based on these surfaces. In Fig. 3(a), the calculated $B(E2,2_1^+ \rightarrow 0_1^+)$ transition probabilities are compared with the experimental values. It is quite evident from the figure that the transition probabilities are well reproduced by the GCM approach. In addition, the ratio $B_{4/2} \equiv B(E2,4_1^+ \rightarrow 2_1^+)/B(E2,2_1^+ \rightarrow 0_1^+)$ and $R_{4/2} \equiv E(4_1^+)/E(2_1^+)$ together with GCM calculations are respectively presented in Figs. 3(b) and 3(c). $B_{4/2}$ ($R_{4/2}$) can be used as an indicator of the nuclear structure, having the value 2 (2) for a pure geometric vibrator [39] and 1.43 (3.33) for an ideal rotor [40]. Due to the transitional character of real nuclei, measured values are expected to lie between these limits. Anomalous $B_{4/2}$ values have once been noticed in ^{180}Pt and turned out to be due to flawed measurement [20]. From Fig. 3(b) it can be found that the $B_{4/2}$ values for most of these Pt isotopes are around 1.8, well above the rotor limit of 1.43. This observation is in accordance with the picture of shape coexistence in these isotopes, which is also suggested by other authors [15,41,42]. In case of shape coexistence, the energy difference between the two minima (the prolate one and the oblate one) increases quickly with spin. For the yrast band, the effect of the oblate minimum attenuates with increasing spin (see Fig. 4), bringing extra enhancement to the $B(E2,4_1^+ \rightarrow 2_1^+)$ values and, therefore, to the $B_{4/2}$ ratio. Recent lifetime measurements of the yrast bands for ^{182,186}Pt [23] isotopes showed a dramatic increase in $B(E2)$ transition probabilities with increasing spin, which had been explained by using the prescription of mixing of two bands corresponding to two different shapes, in general agreement with the interpretation presented here.

However, the observed $B_{4/2}$ value for ^{178}Pt, on the other hand, lies close to the rotor limit, does not seem to follow the smooth trend of data from neighboring isotopes, although the $B(E2,2_1^+ \rightarrow 0_1^+)$ and $R_{4/2}$ values do. The 4_1^+ state lifetime was measured in a single experiment [4] in which it is now well known that effects of level lifetimes involved in side-feeding transitions can give erroneous results. Of course, it could certainly be worthwhile remeasuring with a modern plunger for checking whether an interesting structural effect causes this anomaly or whether the error bars have been underestimated on the data point.

Although the present results may appear to be consistent with the shape-coexistence scenario, there have been some debate regarding whether shape evolution in the Pt isotopes involves intruder configurations [13,14,16] or could be understood without invoking intruder configurations [12]. In Ref. [12] a single-configuration Hamiltonian, in the framework of the IBM, is used to describe the excited states in Pt isotopes with $N > 94$. This approach is in good agreement with experiment without the need to include mixing with an intruder configuration. Moreover, in Refs. [14,16], both single- and configuration-mixing models were shown to give almost equivalent results in a limited set of data. They concluded that, in Pt isotopes, configuration mixing is somehow "hidden" and have suggested further spectroscopic measurements where this mixing might be clearly revealed. In this paper, the agreement between experimental and theoretical values, shown in Fig. 3, is reasonably good with introducing more configurations and our results do support the intuitive shape-coexistence picture for light Pt isotopes.

In summary, the lifetime of the 2_1^+ state in ^{178}Pt was measured in a fast-time experiment to be $\tau = 412\,(30)$ ps. The present experiment provides a result which extends the systematics of $B(E2,2_1^+ \rightarrow 0_1^+)$ values of Pt isotopes. Theoretical calculations in terms of the generator coordinate method are in good agreement with the systematic experimental results. The present results support a configuration-mixing interpretation for low-spin states and provide an important basis for the interpretation and understanding of the shape-coexistence phenomenon in light Pt isotopes. Further experimental work to determine the lifetimes of the high-spin states and side bands will help to further elucidate the nuclear structure in this region.

We would like to thank the HI-13 tandem accelerator staff for the smooth operation of the machine. We are grateful to Dr. Q.W. Fan for his assistance during target preparation. This work was partially supported by the National Natural Science Foundation of China under Contracts No. 10927507, No. 11075214, No. 11375267, No. 11305269, No. 10675171, and No. 11175259.

[1] K. Heyde and J. L. Wood, Rev. Mod. Phys. **83**, 1467 (2011).
[2] J. L. Wood *et al.*, Phys. Rep. **215**, 101 (1992).
[3] K. Heyde *et al.*, Phys. Rep. **102**, 291 (1983).
[4] G. D. Dracoulis *et al.*, J. Phys. G: Nucl. Phys. **12**, L97 (1986).
[5] R. Bengtsson *et al.*, Phys. Lett. B **183**, 1 (1987).
[6] F. G. Kondev *et al.*, Phys. Rev. C **61**, 044323 (2000).
[7] D. G. Popescu *et al.*, Phys. Rev. C **55**, 1175 (1997).
[8] P. M. Davidson *et al.*, Nucl. Phys. A **657**, 219 (1999).
[9] M. K. Harder, K. T. Tang, and P. Van Isacker, Phys. Lett. B **405**, 25 (1997).
[10] S. L. King *et al.*, Phys. Lett. B **443**, 82 (1998).
[11] E. A. McCutchan and N. V. Zamfir, Phys. Rev. C **71**, 054306 (2005).
[12] E. A. McCutchan, R. F. Casten, and N. V. Zamfir, Phys. Rev. C **71**, 061301(R) (2005).
[13] I. O. Morales, A. Frank, C. E. Vargas, and P. Van Isacker, Phys. Rev. C **78**, 024303 (2008).
[14] J. E. García-Ramos and K. Heyde, Nucl. Phys. A **825**, 39 (2009).
[15] K. Nomura, T. Otsuka, R. Rodríguez-Guzmán, L. M. Robledo, and P. Sarriguren, Phys. Rev. C **83**, 014309 (2011).
[16] J. E. García-Ramos, V. Hellemans, and K. Heyde, Phys. Rev. C **84**, 014331 (2011).
[17] A. A. Raduta and P. Buganu, Phys. Rev. C **88**, 064328 (2013).
[18] J. E. García-Ramos, K. Heyde, L. M. Robledo, and R. Rodríguez-Guzmán, Phys. Rev. C **89**, 034313 (2014).
[19] G. D. Dracoulis *et al.*, Phys. Rev. C **44**, R1246 (1991).
[20] E. Williams *et al.*, Phys. Rev. C **74**, 024302 (2006).
[21] Y. Oktem *et al.*, Phys. Rev. C **76**, 044315 (2007).
[22] E. A. McCutchan *et al.*, Phys. Rev. C **78**, 014320 (2008).
[23] J. C. Walpe *et al.*, Phys. Rev. C **85**, 057302 (2012).
[24] K. A. Gladnishki *et al.*, Nucl. Phys. A **877**, 19 (2012).
[25] C. Y. Wu *et al.*, Nucl. Phys. A **607**, 178 (1996).
[26] E. Hagberg *et al.*, Nucl. Phys. A **318**, 29 (1979).
[27] J. Wauters *et al.*, Z. Phys. A: Hadrons Nucl. **345**, 21 (1993).
[28] F. Soramel *et al.*, Eur. Phys. J. A **4**, 17 (1999).
[29] F. Pühlhofer, Nucl. Phys. A **280**, 267 (1977).
[30] C. B. Li *et al.*, Phys. Rev. C **86**, 057303 (2012).
[31] H. Mach, R. L. Gill, and M. Moszyiński, Nucl. Instrum. Methods Phys. Res., Sect. A **280**, 49 (1989).
[32] N. Mărginean *et al.*, Eur. Phys. J. A **46**, 329 (2010).
[33] G. D. Dracoulis, Phys. Rev. C **49**, 3324 (1994).
[34] F. Q. Chen, Y. Sun, and P. Ring, Phys. Rev. C **88**, 014315 (2013).
[35] K. Hara and Y. Sun, Int. J. Mod. Phys. E **04**, 637 (1995).
[36] R. Rodríguez-Guzmán, P. Sarriguren, L. M. Robledo, and J. E. García-Ramos, Phys. Rev. C **81**, 024310 (2010).
[37] G. H. Bhat, J. A. Sheikh, Y. Sun, and U. Garg, Phys. Rev. C **86**, 047307 (2012).
[38] T. Nikšić, D. Vretenar, and P. Ring, Prog. Part. Nucl. Phys. **66**, 519 (2011).
[39] G. Gneuss and W. Greiner, Nucl. Phys. A **171**, 449 (1971).
[40] A. S. Davydov and G. F. Filippov, Nucl. Phys. **8**, 237 (1958).
[41] S. Aberg, H. Flocard, and W. Nazarewicz, Annu. Rev. Nucl. Part. Sci. **40**, 439 (1990).
[42] P. Sarriguren, R. Rodríguez-Guzmán, and L. M. Robledo, Phys. Rev. C **77**, 064322 (2008).